Determination of the mixing matrix and of the pattern of masses

D.Autiero, IPN Lyon

1 Introduction

During the last six years the field of neutrino physics had a quite spectacular development with the confirmation of the interpretation of the atmospheric neutrinos anomaly in terms of neutrino oscillations by the SuperKamiokande and K2K experiments and the final proof that neutrino oscillations are at the origin of the solar neutrino problem by the SNO and Kamland experiments.

Ignoring the LSND result, the experimental data are quite well described by a scenario involving three massive neutrinos with two almost independent oscillations.

Atmospheric neutrinos data are described by a $\nu_\mu \leftrightarrow \nu_\tau$oscillation corresponding to a mass difference Δm^2_{23}= 2.4×10^{-3} eV^2 and an almost maximal mixing angle.

Solar neutrinos are well described in terms of $\nu_\mu \leftrightarrow \nu_e$oscillations by the LMA MSW solution : an overall fit of the solar neutrino data + the Kamland experiments gives Δm^2_{12}= 8.2×10^{-5} eV^2 and a mixing angle θ_{12} which is not maximal [1].

The LSND result is going to be verified by the MiniBoone experiment, in case of confirmation it will imply the existence of a fourth neutrino which is badly compatible with the existing data unless of exotic hypotesis like CPT violation [4].

Under the framework of only 3 neutrinos the mixing matrix linking the flavor eigenstates to the mass eigenstates can be parametrized in terms of 3 angles and one Dirac-like CP phase δ (Pontecorvo-Maki-Nagakawa-Sakata mixing matrix).

$$U \equiv U_{23}U_{13}U_{12} \equiv \begin{pmatrix} 1 & 0 & 0 \\ 0 & c_{23} & s_{23} \\ 0 & -s_{23} & c_{23} \end{pmatrix} \begin{pmatrix} c_{13} & 0 & s_{13}e^{-i\delta} \\ 0 & 1 & 0 \\ -s_{13}e^{i\delta} & 0 & c_{13} \end{pmatrix} \begin{pmatrix} c_{12} & s_{12} & 0 \\ -s_{12} & c_{12} & 0 \\ 0 & 0 & 1 \end{pmatrix} \tag{1}$$

$$U = \begin{pmatrix} c_{12}c_{13} & s_{12}c_{13} & s_{13}e^{-i\delta} \\ -s_{12}c_{23} - c_{12}s_{13}s_{23}e^{i\delta} & c_{12}c_{23} - s_{12}s_{13}s_{23}e^{i\delta} & c_{13}s_{23} \\ s_{12}s_{23} - c_{12}s_{13}c_{23}e^{i\delta} & -c_{12}s_{23} - s_{12}s_{13}c_{23}e^{i\delta} & c_{13}c_{23} \end{pmatrix} \tag{2}$$

where: $s_{ij} \equiv \sin\theta_{ij}$, $c_{ij} \equiv \cos\theta_{ij}$.

In case of Majorana neutrinos the matrix would contain two additional phases which nevertheless have no effects on the oscillations.

The angle θ_{13} is actually unknown, there is just an upper limit of 11 degrees put by the CHOOZ experiment corresponding to $\Delta m^2_{23}= 2.4 \times 10^{-3}\ eV^2$. The two other big unknowns are the sign of Δm^2_{23}(direct or inverted mass hierarchy) and the magnitude of the phase δ.

The propagation of neutrinos trough matter alters the oscillation mechanism due to the process of coherent forward scattering occurring on the electrons present in matter. This process has a neutral current and a charged current contribution. The charged current contribution is there only for ν_e and it introduces an asymmetry among flavors, due to the fact that matters does not contain muons or taus. The Hamiltonian describing three flavor neutrino oscillation in matter, written in the flavour basis, is therefore:

$$H = \frac{1}{2E} U \begin{pmatrix} m_1^2 & 0 & 0 \\ 0 & m_2^2 & 0 \\ 0 & 0 & m_3^2 \end{pmatrix} U^\dagger + \frac{1}{2E} \begin{pmatrix} A + A' & 0 & 0 \\ 0 & A' & 0 \\ 0 & 0 & A' \end{pmatrix}, \tag{3}$$

Where the quantities A and A' describe respectively the charged current and neutral current contributions to the effective potential, with:

$$A = 2\sqrt{2} G_F n_e E \tag{4}$$

For antineutrinos A has to be replaced by -A, so that their behavior in matter differs (matter is not CP invariant).

The effect of the potential is equivalent to a shift in the squared mass of the neutrino:

$$E - V = E - \frac{A}{2E} = \sqrt{p^2 + m^2} \simeq P + \frac{m^2}{2p} \tag{5}$$

by approximating the momentum with the energy one obtains:

$$m^2 \rightarrow m^2 + A \tag{6}$$

In this way electron neutrinos (antineutrinos) acquire a larger (smaller) squared mass:

$$(\Delta m^2)_{matter}{}^{\nu_e(\overline{\nu}_e)} = \pm A \simeq \pm 0.76 \times 10^{-4} (\frac{\rho}{gcm^{-3}})(\frac{E}{GeV})(\frac{Y_e}{0.5}) eV^2 \tag{7}$$

Where ρ and Y_e are respectively the density and number of electrons per nucleon of the matter considered.

The flavor evolution in presence of matter effects is not trivial but it can be solved analitically for the case of constant density by diagonalizing the Hamiltonian. This is done by considering the earth density as constant over baselines up to 1000 Km. For energies comparable to the one corresponding to the first atmospheric oscillation maximum ($|\Delta m^2_{23} L/E| \approx 1$), the effective oscillation parameters in matter will be:

$$
\begin{aligned}
\sin^2\theta_{23}^m(A) &\simeq \sin^2\theta_{23}, && (8)\\
\sin^2 2\theta_{12}^m(A) &\simeq \frac{\Delta m_{12}^2}{\pm A}\sin 2\theta_{12}, && (9)\\
\sin^2 2\theta_{13}^m(A) &\simeq \frac{\sin^2 2\theta_{13}}{C}, && (10)\\
\delta^m &\simeq \delta, && (11)\\
\Delta M_{12}^2 &\simeq \pm A, && (12)\\
\Delta M_{23}^2 &\simeq \Delta m_{23}^2\sqrt{C}, && (13)\\
& && (14)
\end{aligned}
$$

where:

$$C \equiv \sin^2 2\theta_{13} + (\frac{\pm A}{\Delta m_{23}^2} - \cos 2\theta_{13})^2. \tag{15}$$

At the energy (E^{res}) where the MSW resonance occurs the value of $\sin^2 2\theta_{13}$ in matter: $\sin^2 2\theta_{13}^m$ becomes equal to 1, independently of the actual value of this angle in vacuum.

$$E_\nu^{res}(GeV) = \frac{\cos 2\theta_{13}\Delta m_{23}^2}{2\sqrt{2}G_F n_e} \simeq \frac{1.32\times 10^4 \cos 2\theta_{13}\Delta m_{23}^2(eV^2)}{\rho(g/cm^3)} \tag{16}$$

In the earth crust ($\rho = 2.8$ g/cm^3) and for $\Delta m_{23}^2 = 2.5\times 10^{-3}$ eV^2 and $\theta_{13} \ll 1$ the energy of the MSW resonance is 11.8 GeV.

The actual status of knowledge of the parameters of the mixing matrix is summarized in table 1 [3].

parameter	best fit	2σ	3σ	5σ
Δm_{21}^2 [$10^{-5}eV^2$]	6.9	6.1–8.4	5.4–9.4	2.1–29
Δm_{31}^2 [$10^{-3}eV^2$]	2.3	1.4–3.0	1.1–3.4	0.68–4.4
$\sin^2\theta_{12}$	0.30	0.25–0.35	0.23–0.39	0.16–0.47
$\sin^2\theta_{23}$	0.52	0.36–0.66	0.32–0.70	0.26–0.78
$\sin^2\theta_{13}$	0.005	≤ 0.037	≤ 0.061	≤ 0.13

Table 1: Best-fit values, 2σ, 3σ, and 5σ intervals (1 d.o.f.) for the three-flavour neutrino oscillation parameters from global data including solar, atmospheric, reactor (KamLAND and CHOOZ) and accelerator (K2K) experiments.

A remarkable progress for what concern Δm_{12}^2has been recently presented by the Kamland experiment [1] which is now strongly constraining this parameter by the observed energy dependence of disappearance of reactor $\overline{\nu}_e$. When combined with solar neutrino experiments this result yields: Δm_{12}^2= $8.2^{+0.5}_{-0.6}\times 10^{-5}$ eV^2 and $\tan^2\theta_{12} = 0.40^{+0.09}_{-0.07}$.

In the next years the long baseline experiments on the NUMI and CNGS beams will provide the final confirmation of the atmospheric neutrino oscillations, they will also contribute to increase the precision on the $\Delta m^2_{23}$and θ_{23} parameters and they will perform as well searches for $\nu_\mu \leftrightarrow \nu_e$oscillations which could improve the sensitivity on the θ_{13} parameter by about a factor two with respect to the CHOOZ limit. The parameters of the solar sector, which have already a remarkable precision should also improve as well with Kamland statistics and with the start of a new closer (at 88 Km) reactor. Possible improvements on θ_{12} are directly related to solar neutrino experiments.

Given the values of $\Delta m^2_{23}$and Δm^2_{12}, the two oscillations are not completely decoupled but the oscillation probabilities can be developed, in order to simplify the notation and put better in evidence the various effects, in terms of the ratio of the two mass differences $\alpha = \Delta {m^2}_{21}/\Delta {m^2}_{31} \simeq 10^{-2}$. An expression up to the second order in α yields [14, 21–23]:

$$
\begin{aligned}
P_{\nu_\mu \to \nu_e} &\simeq \sin^2 2\theta_{13} \, \sin^2\theta_{23} \frac{\sin^2[(1-\hat{A})\Delta]}{(1-\hat{A})^2} \\
&\pm \alpha \sin\delta \sin 2\theta_{13} \, \cos\theta_{13} \, \sin 2\theta_{12} \, \sin 2\theta_{23} \, \sin(\Delta) \frac{\sin(\hat{A}\Delta)}{\hat{A}} \frac{\sin[(1-\hat{A})\Delta]}{(1-\hat{A})} \\
&+ \alpha \cos\delta \sin 2\theta_{13} \, \cos\theta_{13} \, \sin 2\theta_{12} \, \sin 2\theta_{23} \, \cos(\Delta) \frac{\sin(\hat{A}\Delta)}{\hat{A}} \frac{\sin[(1-\hat{A})\Delta]}{(1-\hat{A})} \\
&+ \alpha^2 \, \cos^2\theta_{23} \sin^2 2\theta_{12} \frac{\sin^2(\hat{A}\Delta)}{\hat{A}^2} \\
&\equiv O_1 \; + \; O_2(\delta) \; + \; O_3(\delta) \; + \; O_4 \quad .
\end{aligned} \tag{17}
$$

Where: $\Delta = \Delta {m^2}_{31} L/4E$ The sign of the term $O_2(\delta)$ is positive for neutrinos and negative for antineutrinos.

Matter effects are included as well through the dimensionless term $\hat{A}$, which represents the ratio between the neutrino energy and the energy (E^{res}) for which the MSW resonance occurs.

$$
\hat{A} \equiv 2\sqrt{2} G_F n_e E / \Delta {m^2}_{31} \tag{18}
$$

with G_F the Fermi coupling constant and n_e the electron density in matter. The sign of $\hat{A}$ depends on the sign of Δm^2_{31} which is positive (negative) for normal (inverted) hierarchy of neutrino masses. Matter effects have opposite sign for neutrinos and antineutrinos and for the normal versus inverted mass hierarchy.

If the experiment is performed in correspondence to the first oscillation peak, the oscillation probability can be approximated by:

$$
{P_{\nu_\mu \to \nu_e}}^{matter} \simeq (1 \pm 2 \frac{E}{E_{res}}) {P_{\nu_\mu \to \nu_e}}^{vacuum} \tag{19}
$$

From which one can see that matter effects increase linearly with the neutrino energy (or with the baseline by imposing the condition to be still at the first maximum) and for normal hierarchy they enhance the oscillation probability for neutrinos, the opposite happens for antineutrinos.

The $\nu_\mu \leftrightarrow \nu_e$formula is composed by four different pieces which have different behaviours in terms of matter effects, CP violating effects and the sign of Δm^2_{31}. The first term ($O_1(\delta)$ is independent on CP and matter effects and it is dominant. The $\nu_\mu \leftrightarrow \nu_e$oscillation rate depends therefore in first order on the value of $\sin^2 2\theta_{13}$, but also on the matter and CP effects.

The terms $O_2(\delta)$ and $O_3(\delta)$ are respectively CP odd and CP even, furthermore they depend respectively on $\sin(\Delta)$ and $\cos(\Delta)$. This means that for an experiment performed at the oscillation peak ($\Delta \simeq \pi/2$) the term $O_2(\delta)$ is larger than $O_3(\delta)$. For an experiment performed off-peak (Δ small), like the experiments at CNGS [14]:

$$\frac{\sin^2[(1-\hat{A})\Delta]}{(1-\hat{A})^2} \simeq \Delta^2 \tag{20}$$

In this case matter effects cancels out and the term $O_3(\delta)$ is larger than $O_2(\delta)$, $O_3(\delta)$ with the characteristics of being CP even and odd under the inversion of the sign of Δm^2_{31}. This is an example on how the study of the $\nu_\mu \leftrightarrow \nu_e$oscillation rate with different choiches of L and E will bring complementary informations on the various parameters affecting the oscillation ($\sin^2 2\theta_{13}$, δ, sign of Δm^2_{31}).

For the study of CP violation one has to measure the $\nu_\mu \leftrightarrow \nu_e$oscillation probabilities for neutrinos and antineutrinos. In the calculation of the asymmetry only the term $O_2(\delta)$ survives and:

$$\frac{P(\nu_\mu \leftrightarrow \nu_e) - P(\overline{\nu}_\mu \leftrightarrow \overline{\nu}_e)}{P(\nu_\mu \leftrightarrow \nu_e) + P(\overline{\nu}_\mu \leftrightarrow \overline{\nu}_e)} \simeq \frac{2 \times O_2(\delta)}{O_1(\delta)} \tag{21}$$

Neglecting matter effects one obtains:

$$\frac{P(\nu_\mu \leftrightarrow \nu_e) - P(\overline{\nu}_\mu \leftrightarrow \overline{\nu}_e)}{P(\nu_\mu \leftrightarrow \nu_e) + P(\overline{\nu}_\mu \leftrightarrow \overline{\nu}_e)} \simeq \frac{\Delta m^2_{12} L}{4E} \frac{\sin 2\theta_{12}}{\sin \theta_{13}} \sin \delta \tag{22}$$

Given the complex dependence of the oscillation probability on the various parameters, a measurement of the appearance probability $P_{\alpha\beta}(\bar{\theta}_{13}, \bar{\delta})$ for neutrinos at a given energy and distance will not provide as unique solution the true values $(\bar{\theta}_{13}, \bar{\delta})$ but a locus of points (θ_{13}, δ) [16–19,22]. The aspect of degeneracies is very important to plan future experiments which should disentangle the effects of the single oscillation parameters and provide precision measurements of each one of them.

In order to disentangle correlations and degeneracies it is needed to combine informations of complementary experiments (studying different channels, at different energies or baselines, with different impact of matter effects and the CP phase) and/or complementary informations within the same experiment (for instance different bins in the neutrino energy). This as a strong impact in planning future facilities and also the experimental techniques which should be used, since these are depending on the energy range and the channels to be studied.

The first kind of degeneracy arises when mapping the $\nu_\mu \leftrightarrow \nu_e$appearance probability on the plane (θ_{13}, δ). The four terms of the equation can be syntetically written as follows for small values of θ_{13}:

$$P(\nu_\mu \leftrightarrow \nu_e) \simeq {\theta_{13}}^2 \times C_1 + \theta_{13} \times (\pm \sin\delta C_2 + \cos\delta C_3) + C_4 \tag{23}$$

The bound $P(\nu_\mu \leftrightarrow \nu_e) = constant$ leads for neutrinos and antineutrinos to two independent loci of correlated solutions. The two curves for neutrinos and antineutrinos will cross in the point corresponding to the true solution and, depending on L and E, in another point called "intrinsic clone". This degeneration can be solved by repeating the measurements at a different energy/baseline.

Another degeneracy comes from the ignorance of the sign of Δm^2_{31}. A change in this sign can be compensated by a variation in δ. The change of the sign of Δm^2_{31} implies in the equation of $P(\nu_\mu \leftrightarrow \nu_e)$: $\alpha \to -\alpha$, $\Delta \to -\Delta$, $\hat{A} \to -\hat{A}$. The terms $O_2(\delta)$ and $O_3(\delta)$ are not invariant under this transformation which can be compensated by a change in δ

The third degeneracy comes from the fact that the angle θ_{23} is known to be close to 45 degrees but it is not know if it is greater or smaller than 45 degrees. The terms $O_2(\delta)$ and $O_3(\delta)$ are not invariant under the transformation $\theta_{23} \to \pi/2 - \theta_{23}$. This transformation can be reabsorbed by a small shift in the (θ_{13}, δ) parameters yielding another solution called "octant clone".

Putting all these possibilities togheter one arrives to an eigth-fold degeneracy, which will be present in case $P(\nu_\mu \leftrightarrow \nu_e)$ and $P(\overline{\nu}_\mu \leftrightarrow \overline{\nu}_e)$ are measured at the same energy and baseline. The parameters can be disentagled by using measurements at different L or E or by studying other oscillation channels like $P(\nu_e \leftrightarrow \nu_\tau)$.

The measurements at different energies can be obtained by using a wide band beam by the same experiment depending on its capability and resolution in reconstructing the neutrino energy. An appearance experiment just measuring the $P(\nu_\mu \leftrightarrow \nu_e)$ oscillation rate without reconstructing any information on the neutrino energy can be called "counting experiment".

The considerations made so far on the degeneracies and correlations will affect, at various stages of the future experimental strategy on the determination of the mixing matrix, first the experiments aimed at measuring a finite value of θ_{13}, then the ones aiming to a first evidence for CP violation and finally the precision individual measurement of the elements of the mixing matrix. Sometimes these correlations may be taken as limiting aspects of a single measurements but in other cases they can be exploited in order to get a synergy of different experiments.

We can outline the future activity on the determination of the elements of the mixing matrix in 4 phases:

- Current experiments The already approved longbaseline experiments (2001-2010) (K2K, MINOS, CNGS) will attempt for a first search for $\nu_\mu \leftrightarrow \nu_e$oscillations, which can improve the CHOOZ limit by a factor 2 and detect the oscillations for $\theta_{13} \gtrsim 7^\circ$

- Next generation The next generation of experiments (2009-2015)with superbeams (T2K, NOVA) and new experiments at reactors (Double CHOOZ, Diablo Canyon,) aims to improve the CHOOZ limit by a factor 20. They will improve the knowledge of the atmospheric neutrino parameters. They will have a very limited sensitivity of the CP phase, also combining their results.

- First CP violation experiments (2015-2025) They will aim at a first evidence for CP violation. To be performed by using superbeams and/or betabeams coupled with water Cerenkov detectors of 1 Mton (HyperKamiokande, Frejus), they will reach a sensitivity on θ_{13} about 200 times better than the CHOOZ limit.

- Precision measurements ($\geq$ 2020) Neutrino factories and/or betabeams. These facilities should provide precision measurements of the mixing parameters and determine the mass hierarchy.

2 Current longbaseline experiments

The current generation of longbaseline experiments (K2K, MINOS, CNGS) is aiming to a final confirmation of neutrino oscillations for atmospheric neutrinos and to measure the oscillation parameters θ_{23} and Δm^2_{23}. The K2K experiment, is looking at the $\nu_\mu$disappearance over a baseline of 250 Km with a two detector setup, where the far detector is SuperKamiokande. It has already reached a statistical significance of 3.9 σ by combining the measured event rate and the spectral distortion [2]. MINOS will start in 2005 and, still by looking at the $\nu_\mu$disappearance with neutrinos of a few GeV over 730 Km baseline should be able to measure Δm^2_{23} with a 10% accuracy.

The CNGS program (OPERA and ICARUS) is going to start in 2006 and will look for $\nu_\tau$appearance. Both the CNGS experiments and MINOS are sensitive to θ_{13} by performing a $\nu_\mu \leftrightarrow \nu_e$oscillation search and are going to improve significatively with respect to the CHOOZ limit (by a factor 2 or 3 within 2009). As shown before, their sensitivities have complementary aspects [14, 31]. The CNGS experiments, due to the high energy needed for $\nu_\tau$appearance, will be performed at a off-peak baseline with a partial cancellation of matter effects and with the oscillation probability affected mostly by terms CP even and odd under the inversion of the sign of Δm^2_{31}. In MINOS matter effects are of the order of 20% and the ignorance of the sign of Δm^2_{23} introduces a degeneracy in the θ_{13} sensitivity if the experiment is considered as stand-alone. This can be also used in a synergic way by combining with other experiments with a complementary behavior. The sensitivity of this generation of experiment can go down to about 5°. For values of θ_{13} greter than 7° CNGS could be able to establish an evidence of $\nu_\mu \leftrightarrow \nu_e$oscillations at 3 σ level independently of the value of δ_{CP} [15].

For a real measurement of θ_{13} one will have to wait for the next generation of experiments. A summary of the θ_{13} exclusion sensitivities at 90% CL of the current experiments is shown in table reft13current, for CGNS the results obtainable with the beam upgrade ($\times 1.5$) currently under study are reported as well.

Experiment	$\sin^2(2\theta_{13}$	θ_{13}
MINOS 2yr	≤ 0.06	$\leq 7.1°$
ICARUS 5yr	≤ 0.04	$\leq 5.8°$
beam $\times 1.5$	≤ 0.03	$\leq 5°$
OPERA 5yr	≤ 0.06	$\leq 7.1°$
beam $\times 1.5$	≤ 0.05	$\leq 6.4°$
ICARUS+OPERA 5yr	≤ 0.03	$\leq 5°$
beam $\times 1.5$	≤ 0.025	$\leq 4.5°$

Table 2: Comparison θ_{13} sensitivities at 90% CL of the current longbaseline experiments

3 Next generation experiments

The next generation of longbaseline experiments is designed with the purpose of performing a $\nu_\mu \leftrightarrow \nu_e$oscillation search with a significative increase in sensitivity with respect to CHOOZ (about a factor 20). In order to achieve this goal the experiments plan to study the $\nu_e$appearance with a beam tuned at the first oscillation maximum. This is obtained by using low energy, high intensity narrow-band beams with a low $\nu_e$contamination coupled to high detector masses. The main characteristics of these beams with respect to the ones planned for current experiments are outlined in Table 3.

	T2K	NOVA	MINOS	ICARUS	OPERA
Baseline (km)	295	810	735	732	732
Mean energy (GeV)	0.76	2.22	3	17	17
Exposure (kton×years)	22.5×5	17×5	5.4×2	2.4×5	1.7×5
L/E (km/GeV)	388	321	245	43	43

Table 3: Main parameters of the current and next future long baseline experiments.

Both the T2K and NOVA projects [27, 28] are based on Off-Axis beams. The Off-Axis concept is based on the fact that for small angles, the flux and energy of a neutrino produced from the two body decay of a pion in flight are given in the lab frame by:

$$\mathcal{F} = \left(\frac{2\gamma}{1+\gamma^2\theta^2}\right)^2 \frac{A}{4\pi z^2}, \;\; E_\nu = \frac{0.43 E_\pi}{1+\gamma^2\theta^2}, \tag{24}$$

where θ is the angle between the pion direction and the neutrino direction, E_π is the energy of the parent pion, and m_π is the mass of the pion and $\gamma = E_\pi/m_\pi$. A and z are the detector cross-sectional area and distance from decay point.

As can be seen in the Figure 1, the neutrino flux peaks in the forward direction for all values of E_π; As the angle to the beam direction increases, however, the relationship (which is linear at zero degrees) between the pion energy and neutrino energy flattens, with all pions yielding neutrinos of roughly the same energy.

By viewing a conventional beam from a location off the beam axis it is therefore possible to build a a nearly mono-energetic neutrino beam Figure 2 shows the neutrino spectra of the NuMI neutrino beam at locations 5, 10, and 20 km (corresponding to the decay angles of 7, 14, and 21 mrad) off the NuMI beam axis at a distance of 735 km from the target [28]. As can be seen in Fig. 2, it is possible to increase the neutrino yield in the 1-2 GeV region by placing the detector off the beam axis, while at the same time reducing the high-energy component of the neutrino beam and therefore $\nu_e$contamination and its uncertainty in the peak region.

The T2K project is planning, during its first phase, to shoot on the SuperKamiokande detector a superbeam obtained from the 50 GeV proton synchroton (0.75 MW power) of the JPARK accelerator facility. The detector will be 2 degrees off-axis with a baseline of 295 Km and the mean neutrino energy will be 0.76 GeV. Matter effects at this energy are negligible

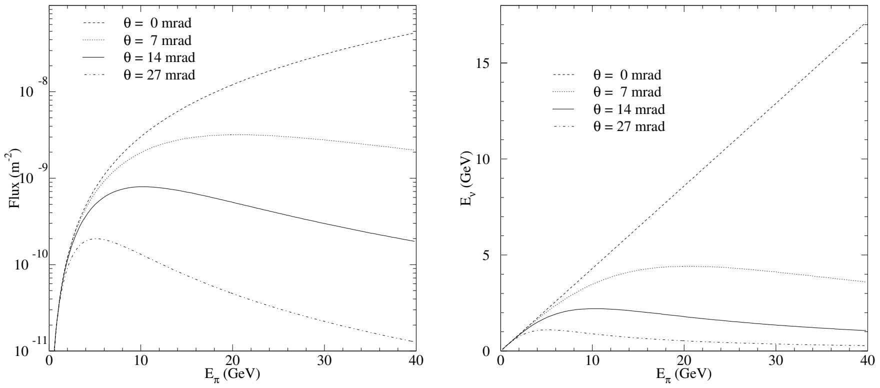

Figure 1: Left: The neutrino flux from a pion of energy E_π as viewed from a site located at an angle θ from the beam axis. The flux has been normalized to a distance of z=735 km. Right: The energy of the neutrino produced at angle θ relative to the pion beam direction as a function of the pion energy.

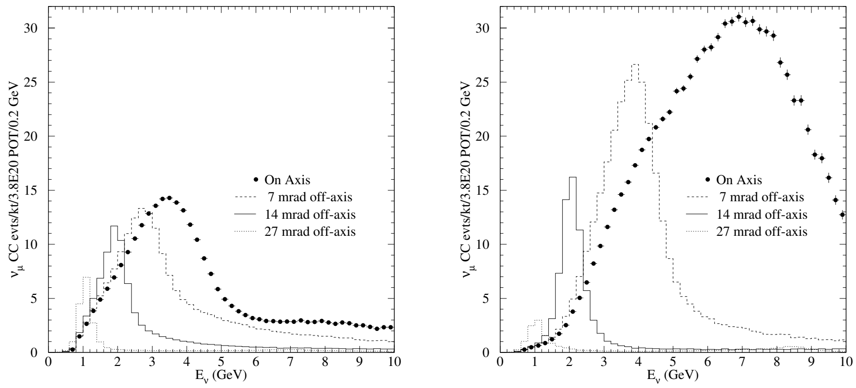

Figure 2: CC muon neutrino events rates expected under 'no oscillation' hypothesis at a distance of 735 km from Fermilab and at various transverse locations for the NuMI low-energy beam configuration (left) and medium-energy beam configuration(right).

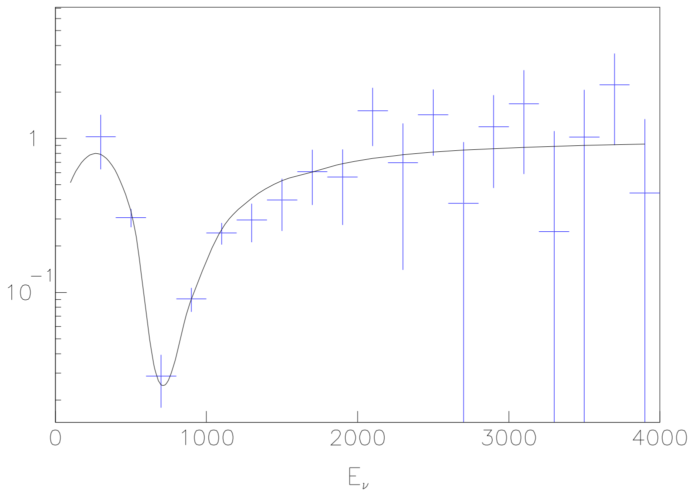

Figure 3: The ratio of the measured spectrum of ν_μ CC in T2K with neutrino oscillation to the expected one without neutrino oscillation after subtracting the contribution of non QE-events. The fit result of the oscillation is superimposed

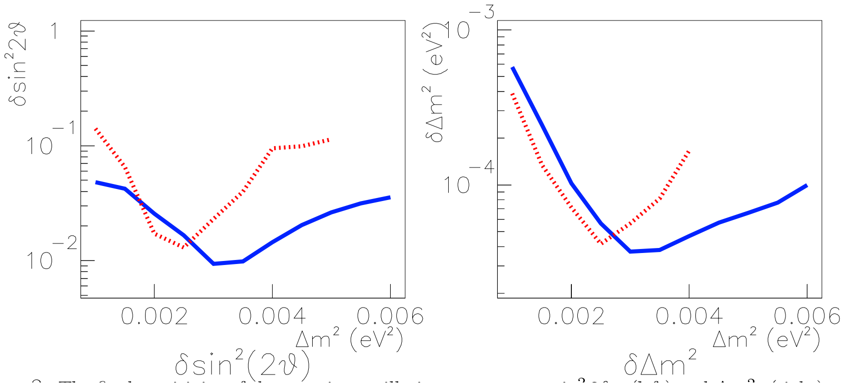

Figure 4: The final sensitivity in T2K phase I of the neutrino oscillation parameters: $\sin^2 2\theta_{23}$ (left) and Δm_{23} (right), as a function of true Δm_{23} (eV^2). The $\sin^2 2\theta_{23}$ is set to 1.00. The result with OA2° is shown by the blue (solid) line, OA3° by the red (dashed) line

(around 10 %) and the $\nu_e$contamination will be at the level of 1 %.

This setup will allow over 5 years of data-taking to improve the CHOOZ limit by a factor 20, extending the search down to $\sin^2 2\theta_{13} \simeq 0.006$ Fig. 5. It will also provide precision measurements of the atmospheric neutrino parameters (Δm^2_{23} with an uncertainty of 10^{-4} eV^2 and $\sin^2 2\theta_{23}$ with an uncertainty of 0.01) Figs. 3,4 and to look for sterile components in $\nu_\mu$disappearance. The project is already approved and data-taking should start in 2009.

The NOVA project [28] will use as neutrino target a 50 Kton low-Z calorimeter located on

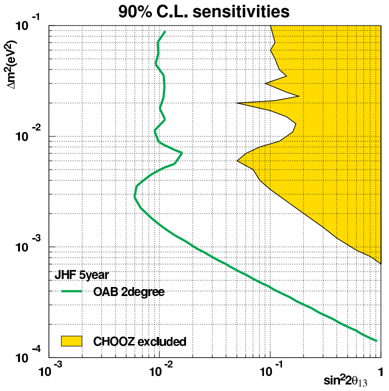

Figure 5: The 90% C.L. sensitivity contours in 5 years of operation of T2K with OA2°. The 90% C.L. excluded region of CHOOZ in plotted in yellow for comparison. $\sin^2\theta_{23}$ is assumed to be 0.5 and the possible contribution due to θ_{12} term is assumed to be small compared to the one due to the θ_{13} term.

the NUMI beam line at a baseline of 810 Km, 0.7 degrees off-axis. The average neutrino energy will be 2.2 GeV, at the peak of the muon rate the $\nu_e$background is at the level of 0.5%. Matter effects are of the order of 23% enhancement (or suppression) of the oscillation probability. The experiment is not approved yet and it could eventually start data-taking by 2010. The experiment aims to a sensitivity to θ_{13} a factor 10 better than MINOS $\sin^2\theta_{13} \leq 0.01$ and to measure $\sin^2\theta_{23}$ with 2% accuracy. The presence of matter effects can be used to attempt a determination of the sign of Δm^2_{23}.

The interplay between CP violation and matter effects is illustrated in figure 6, where the $\sin^2 2\theta_{13}$ is plotted versus the $\overline{\nu}_\mu \leftrightarrow \overline{\nu}_e$oscillation probability for a given value of the $\nu_\mu \leftrightarrow \nu_e$oscillation probability. Measurements of the two probabilities yield an ambuiguity on $\sin^2 2\theta_{13}$ given the presence of CP violating and matter effects. The situation could be disentangled by combining with T2K or with a further measurement performed at the second oscillation maximum.

The mass hierarchy could perhaps be resolved in NOVA for large values of $\sin^2 2\theta_{13}$. A further extension of the sensitivity would need a substantial beam intensity increase which should be provided by a new proton driver, see Fig. 7 .

The parameters $\sin^2 2\theta_{13}$, δ and the sign of Δm^2_{23} all affect in a significant way the $\nu_\mu \leftrightarrow \nu_e$oscillation rate at the atmospheric neutrinos oscillation length. Due to the correlation between δ and $\sin^2 2\theta_{13}$ a large value of δ could even decrease the $\nu_\mu \leftrightarrow \nu_e$oscillation probability being at the origin of a negative result on the search for $\nu_\mu \leftrightarrow \nu_e$oscillations at the next generation of experiments. Single experiments may be limited by the presence of correlations and degeneracies in the measurement of $theta_{13}$, this aspect can be turned to be synergic when experiments with complementary behavior with respect to CP and matter effects are combined togheter in order to better disentangle the various components of the $\nu_\mu \leftrightarrow \nu_e$oscillation probability. The possible synergy among the T2K programme run in neutrino mode (5 years) and the NOVA programme run in antineutrino mode (5 years) can be well appreciated in figure 8 for both signs of the mass hierarchy.

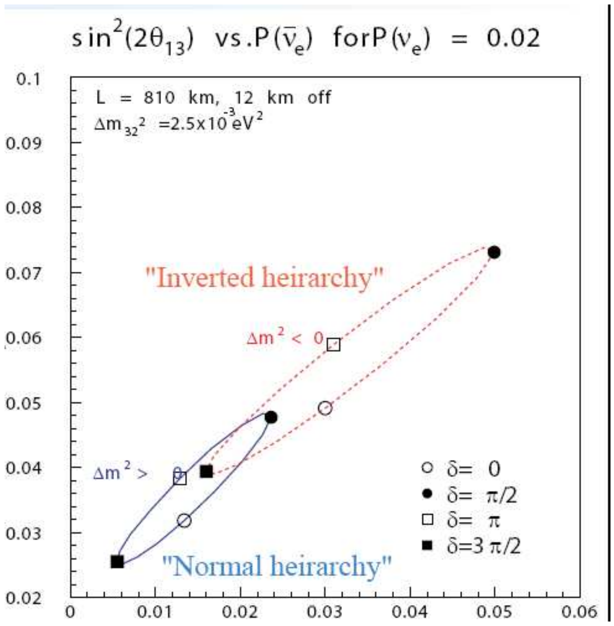

Figure 6: Interplay between CP violation and matter effects in NOVA in the ambiguity for the determination of $\sin^2 2\theta_{13}$. $\sin^2 2\theta_{13}$ is plotted versus the $\overline{\nu}_\mu \leftrightarrow \overline{\nu}_e$oscillation probability for a given value of the $\nu_\mu \leftrightarrow \nu_e$oscillation probability

The sgn(Δm^2_{31})-degeneracy [24], especially for large values of Δm^2_{12}, generates clone solutions at different values of δ. This makes the mass hierarchy a difficult parameter to determine for future longbaseline experiments. The sensitivity to sgn(Δm^2_{31}) can be defined as the capability of excluding the opposite sign at a given confidence level (e.g. 90 %). This is shown for various combinations future experiments in fig. 9 [24]. It can be shown that neither the first-generation superbeams (T2K, NOVA at NUMI), nor their combination, are sensitive to the mass hierarchy [34]. By increasing matter effects in NUMI with a longer baseline (890 Km) at an off-axis angle of 0.72°, and by combining the two Superbeams in order to resolve degeneracies the sensitivity to the sign of Δm^2_{31}can be extended to a large region of the $\sin^2 2\theta_{13}$-Δm^2_{12}-plane [34, 35], which is limited at large values of $\Delta m^2_{12}$by the sgn(Δm^2_{31})-degeneracy. This can be further improved by the combination with a second generation reactor experiment giving a sensitivity independent of $\Delta m^2_{12}$for $\sin^2 2\theta_{13} \geq 0.05$. The same effect is not obtained by combining just the NUMI off-axis with the reactor experiment.

The Double-CHOOZ project is an example of second generation reactor experiments, as well as other projects like Diablo-Canyon and Kashiwasaki [25, 26]. It is aiming to improve the sensitivity of the former CHOOZ experiment by using a two detector setup. This would allow to reduce the systematic uncertainties, which in the old CHOOZ experiment amounted to 2.7%, by canceling out the part related to the knowledge of the neutrino flux from the reactors (1.9%). A further improvement is obtained by reducing the systematic uncertainties related to the detector efficiency (from 1.5% to 0.5%). The far detector would be put in correspondence to the former

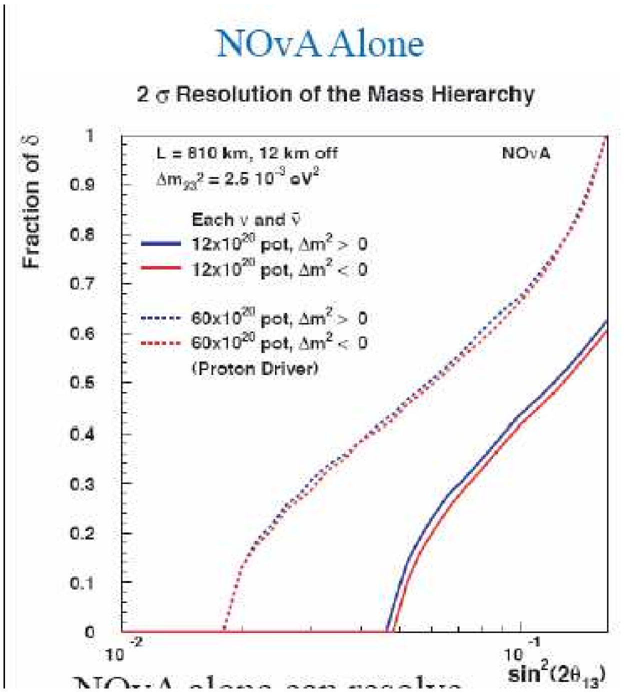

Figure 7: 2 σ resolution of the mass hierarchy contour in NOVA standalone as a function of δ and $\sin^2 2\theta_{13}$.

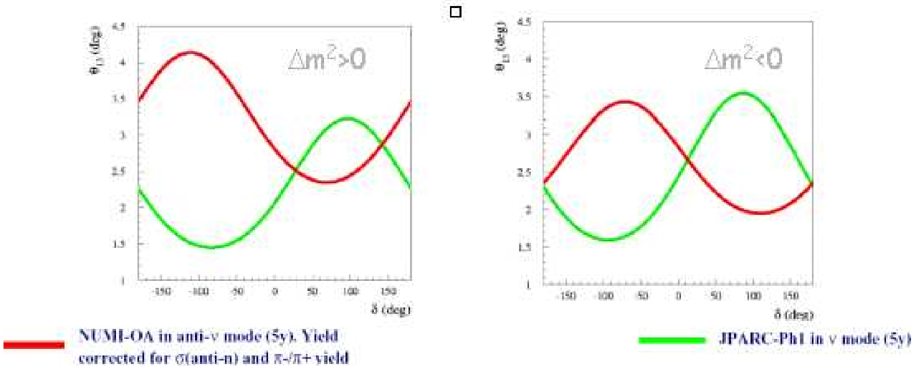

Figure 8: Synergy with respect to the θ_{13} δ_{CP} correlation among the T2K programme run in neutrino in neutrino mode and the NOVA programme run in antineutrino mode. The sensitivity curves at 90% CL fro the two experiments are superimposed for the two values of the sign of Δm^2_{23}clearly showing a complementary behavior with respect to the θ_{13} δ_{CP} correlation.

CHOOZ detector but it is foreseen to be about 2.5 times larger. The near detector, as much as possible similar to the far detector until the PMT surface, would be located under a shielding of 60-80 m.w.e. The realtive normalization error among the two detectors is assumed to be under

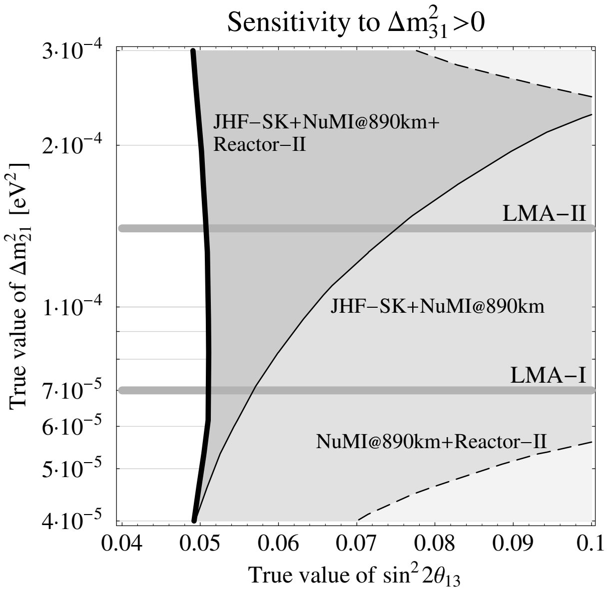

Figure 9: The sensitivity to a positive sign of Δm^2_{31}(normal mass hierarchy) as function of the true values of $\sin^2 2\theta_{13}$ and Δm^2_{12}within the KamLAND-allowed region. The region with a 90% confidence level Sensitivity is located at the the right-hand sides of the curves. It is shown for several combinations of experiments: for T2K combined with NOVA at a baseline of 890 Km, for NOVA at a baseline of 890 Km combined with a second generation reactor experiment, and for T2K combined with NOVA at a baseline of 890 Km and with the reactor experiment. The LMA best-fit values correspond to the horizontal graylines.

control at the level of 0.6 % and the background in both locations is assumed to be less than 1% of the signal. The advantage of a new reactor measurement is that it would be completely independent of the CP phase and matter effects, thus bringing a complementary information in order to solve the correlations and degeneracies in the measurements performed in longbaseline experiments. With an exposure time of 3 years Souble-CHOOZ is foreseen to reach a sensitivity of $\sin^2 2\theta_{13} \leq 0.03$ at 90% C.L. for Δm^2_{23}= $2.0 \times 10^{-3} eV^2$

In order to understand how the combination of the various experiments plays on the determination of CP violation, we define the sensitivity as the 90% confidence level capability of distinguishing $\delta = \pi/2$ from $\delta = 0$. The sensitivity will be limited by degeneration effects due to clone solutions with $\delta = 0$ compatible with the set of measurements corresponding to $\delta = \pi/2$. For the detection of CP violation [34, 35] with superbeams a combined neutrino and antineutrino running is mandatory within one superbeam experiment or in the combination of different superbeams with different polarities. The antineutrino mode, given the smaller cross-section, however has the disadvantage of needing a much longer running time in order to achieve a statistical significancy similar to the one of the neutrino run. The $\sin^2 2\theta_{13}$-δ correlation could be resolved as well by obtaining a precision measurement of $\sin^2 2\theta_{13}$ with a reactor experiment. These possibilities are discussed in fig. 10 where the sensitivity as a function of $\sin^2 2\theta_{13}$ and

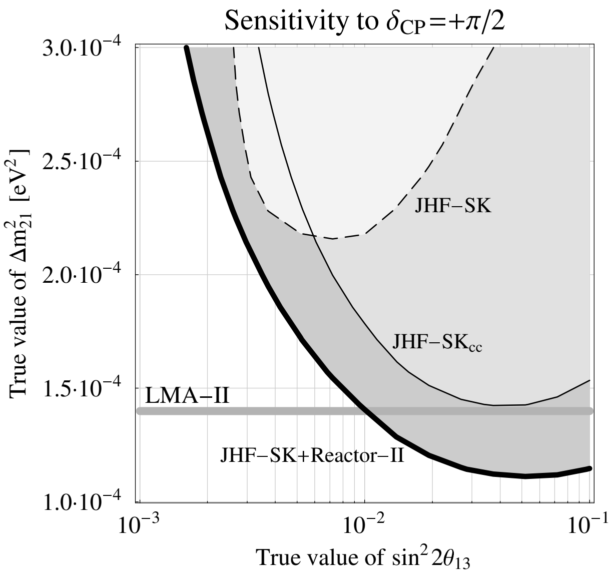

Figure 10: The sensitivity to maximal CP violation $\delta = +\pi/2$ as function of the true values of $\sin^2 2\theta_{13}$ and Δm^2_{12}within the KamLAND-allowed region. The sensitivity region at 90% confidence level corresponds to the upper sides of the curves. It is shown for T2K (neutrino running only), T2K$_{cc}$ (same overall running time split into neutrino and antineutrino running with about equal numbers of events), and T2K (neutrino running only) combined with a second generation reactor experiment. The LMA-II best-fit value corresponds to the horizontal gray line.

$\Delta m^2_{12}$is shown for T2K running with only neutrinos, T2K with equal statistics of neutrinos and antineutrinos and the combination of T2K with neutrinos with a reactor experiment. When the reactor experiment is added to the T2K result with neutrinos and antineutrinos the improvement is just marginal since the $\sin^2 2\theta_{13}$-δ correlation is already sufficiently disentangled by the combination of neutrinos and antineutrinos. The combination of T2K neutrinos with the reactor experiment yields the optimal results given the fact that the T2K statistics is larger than the one obtained in a comparable amount of time by the combined neutrino-antineutrino running modes. The combination with the NOVA experiment does not yield better results given the fact that for NOVA the relative weight of the second and third CP-sensitive terms is lower than in the T2K case.

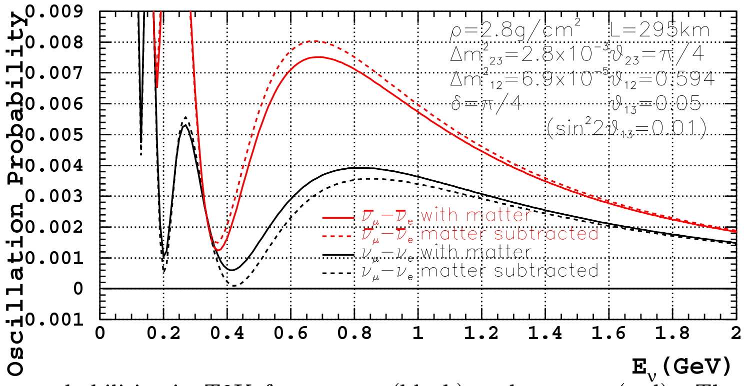

Figure 11: Oscillation probabilities in T2K for $\nu_\mu \leftrightarrow \nu_e$(black) and $\overline{\nu}_\mu \leftrightarrow \overline{\nu}_e$(red). The solid curves include asymmetry due to matter effects. For the dashed curves, the matter effect is subtracted and the difference between $\nu_\mu \leftrightarrow \nu_e$(black) and $\overline{\nu}_\mu \leftrightarrow \overline{\nu}_e$(red) is only due to CP violating effects.

4 First CP violation experiments

In case of observation of $\nu_\mu \leftrightarrow \nu_e$oscillations the T2K project foresees a second phase aiming to the search for a first evidence for CP violation, relying on a sufficently large value of $\sin^2 2\theta_{13}$. This second phase will imply the upgrade of the JPARC 50 GeV PS to a power of 4 MW and the construction of a new large mass water Cerenkov detector (HyperKamiokande) to be used as neutrino target. The beam upgrade $\times 5$ and the detector mass increase $\times 25$ with respect to SuperKamiokande, will provide a statistics increase of a factor 100 with respect to the first phase of T2K. Given the low neutrino energy matter effects have a negligible interference with CP violating effects.

In Europe [8] a project similar to the phase II of HyperKamiokande is actually under study. It is based on the future Superconductive Proton Linac to be built at CERN. This machine would be able to produce a proton beam at an energy of 2.2 GeV and with a power of 4 MW and a total number of protons on target of 10^{23}/year. The SPL is intended to be the proton driver for neutrino factories. The neutrino beam will have an average energy of 270 MeV with the first oscillation maximum at a distance of about 130 Km, corresponding to the distance between CERN and the Frejus underground laboratory. Here, in an future major extension of the already existing laboratory, a large water Cerenkov detector with a fiducial mass of 440 kton could be installed in order to study $\nu_\mu \leftrightarrow \nu_e$oscillations. This detector, like HyperKamiokande, would also be exploitable for an additional physics programme based on the search for proton decay and the study of atmospheric and supernovae neutrinos.

The SPL-Frejus programme would be able to explore θ_{13} down to 1 degree i.e. a factor 100 better than the CHOOZ limit. The intrinsic $\nu_e$contamination of the beam is around 0.4%, coming only from decays of muons, and it can be monitored with a 2% systematic error by using a close detector which will be needed as well to measure the interaction cross-sections which have large uncertainties at the present level of knowledge.

The search for CP violation would imply running the SPL in neutrino and antineutrino mode. Due to the antineutrino interaction cross-section which is about a factor five smaller at

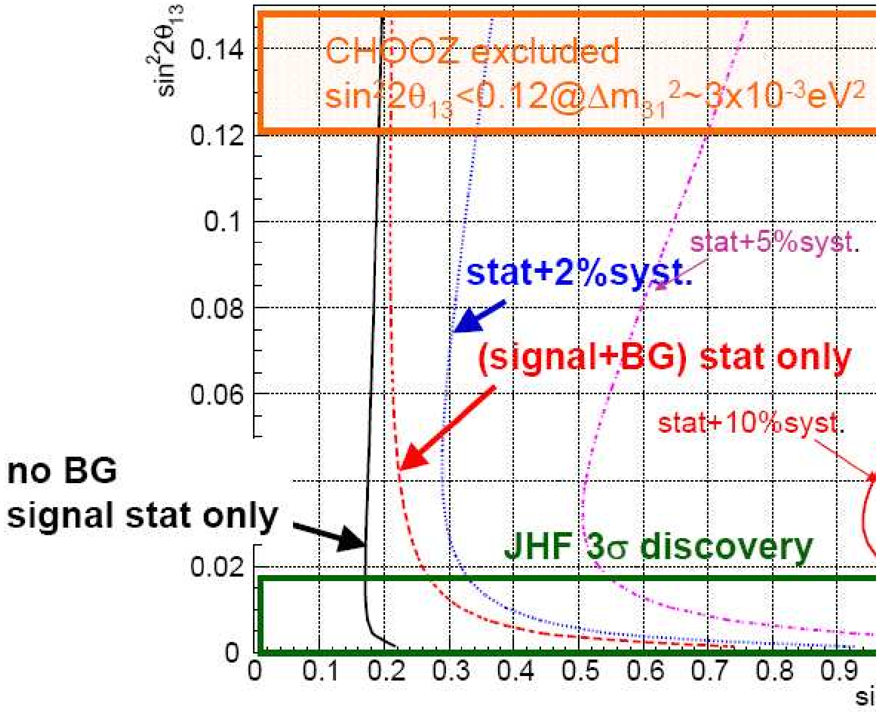

Figure 12: Expected 3σ discovery region of $\sin\delta$ as a function of $\sin^2 2\theta_{13}$ with two years of neutrino running and six years of antineutrino running. The blues dashed curve corresponds to the statistical uncertainties and systematic uncertainties of 2% on the background subtraction.

these energies than the one for neutrinos and due to the smaller production rate of π^- at the beam target, in order to achieve equivalent statistics, 2 years of neutrino running would have to be accompanied by 8 years of antineutrino running. Another feature of this energy domain is that the reconstructed event energy is largely spoiled by Fermi motion so that the measurement performed with the water Cerenkov detector is essentially equivalent to a counting experiment with identification of the final state charged lepton (muon or electron) but without any information on the neutrino energy which, as seen in the Introduction is an essential information in order to resolve degeneracies.

This facility can be more advantagiously exploited by the beta-beam [6,7], which is a pure, intense and well collimated $\nu_e(\overline{\nu}_e)$ beam. This can be obtained by producing, collecting, accelerating to energies with γ factor around 100 and storing in a final decay ring radioactive ions. The best ion candidates, which are required to be easy to produce and with a lifetime around 1 second, are ^{18}Ne for $\nu_e$and ^6He for $\overline{\nu}_e$. On the basis of the ion beams expertise already present at CERN, the beam setup could be assembled by using by recycling in part old equipments like the PS and SPS and by installing a ion production targets fed by the SPL with about 5(matching the SPS) and straight sections of 2500 m each (36%). The final stage acceleration performed with the SPS limits the gamma of the ions to about 150. By matching the magnetic rigidity of the ions injected in the decay ring, the $\nu_e(\overline{\nu}_e)$ beam could be produced at the same time. Given the decay ring constraint: $\gamma(^6\mathrm{He})/\gamma(^{18}\mathrm{Ne}) = 3/5$ the optimal γ values result to be $\gamma(^6\mathrm{He}) = 60$

and $\gamma(^{18}\text{Ne}) = 100$.

Assuming a flux of $2.9 \cdot 10^{18}$ ^{6}He decays/year and $1.1 \cdot 10^{18}$ ^{18}Ne decays/year, the BetaBeam neutrino fluxes at the Frejus detector location, as well as the ones obtainable with the SPL superbeam, are shown in figure Fig. 13. The mean neutrino energies of the $\overline{\nu}_e$, ν_e beams are 0.24 GeV and 0.36 GeV respectively.

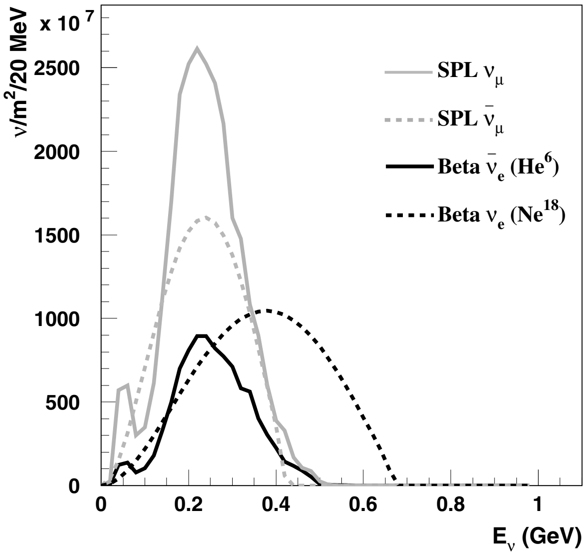

	Fluxes $\nu/m^2/yr$	$\langle E_\nu \rangle$ (GeV)
$\overline{\nu}_e(\gamma = 60)$	$1.97 \cdot 10^{11}$	0.24
$\nu_e(\gamma = 100)$	$1.88 \cdot 10^{11}$	0.36
ν_μ	$4.78 \cdot 10^{11}$	0.27
$\overline{\nu}_\mu$	$3.33 \cdot 10^{11}$	0.25

Figure 13: Beta Beam fluxes at the Frejus location (130 km baseline). The SPL Super Beam ν_μ and $\overline{\nu}_\mu$ fluxes are shown as well in the plot.

Differently with respect to conventional neutrino beams Beta Beams are pure $\nu_e$beams with no intrinsic contamination from other flavors. The search for $\nu_e \rightarrow \nu_\mu$ oscillations would be based on the $\nu_\mu$appearance. At these energies the $\nu_\mu$charge current interactions are mainly quasi-elastic which would appear in the detector as a single ring muon-like events. The background is related to inefficiencies in particle identification, such as mis-identification of pions produced in neutral current single-pion resonant interactions, electrons (positrons) mis-identified as muons. Atmospheric neutrino interactions can also constitute a background which can be reduced by exploiting the time correlation with the parent ion bunches in the decay ring, which will have a length of 10 ns.

Pion production has a threshold at neutrino energies of about 450 MeV, and is strongly suppressed considering the beam spectrum corresponding to this Beta Beam option. The electron background is almost completely suppressed by the request of the detection of a delayed Michel electron following the muon track. In both cases of the superbeam and Beta Beam it is assumed that a 1 *Kton* close detector at 1 *Km* distance would allow to measure precisely the beam and cross sections allowing to achieve a systematic uncertainty of 2%. The synergy among the Superbeam and the Beta Beam, run in parallel, would offer the opportunity of performing searches for CP, T and CPT violation.

Table 4: Event rates for a 4400 kt-y exposure. The signals are computed for $\theta_{13} = 3°$, $\delta = 90°$ sign$(\Delta m^2) = +1$. "δ-oscillated" events indicates the difference between the oscillated events computed with $\delta = 90°$ and with $\delta = 0$. "Oscillated at the Chooz limit" events are computed for $\sin^2 2\theta_{13} = 0.12$, $\delta = 0$.

	Beta Beam		SPL-SB	
	$^6He(\gamma = 60)$	$^{18}Ne(\gamma = 100)$	ν_μ(2 yrs)	$\overline{\nu}_\mu$(8 yrs)
CC events (no osc, no cut)	19710	144784	36698	23320
Oscillated at the Chooz limit	612	5130	1279	774
Total oscillated ($\delta = 90°$, $\theta_{13} = 3°$)	44	529	93	82
δ oscillated	-9	57	-20	12
Beam background	0	0	140	101
Detector backgrounds	1	397	37	50

Signal and background rates for a 4400 kt-yr exposure to ^{6}He and ^{18}Ne beams, together with the SPL SuperBeam (SPL-SB) fluxes [8], are reported in table 4

The sensitivity of this experiment can be expressed in the (θ_{13}, δ) plane, having fixed all the other parameters ($\delta m^2_{23} = 2.5 \cdot 10^{-3}$ eV^2), as shown in Fig. 14-rigth). In the same plot the sensitivity of the SPL-SB computed for a 5 yrs $\nu_\mu$run is displayed . It can be noted the very large variation of the SPL-SB sensitivity for the different values of δ, characteristic of the single flavour run. The BetaBeam, having both CP neutrino states in the same run, exhibits a much more favourable dependence to the CP phase δ.

The search for CP violation can be performed by running the Beta Beam with ^{18}Ne and ^{6}He, and fitting the number of muon-like events to the $p(\nu_e \to \nu_\mu)$ and to the p$(\overline{\nu}_e \to \overline{\nu}_\mu)$ probabilities. The fit can simultaneously determine θ_{13} and δ, see fig. 17.

The region of 99% CL sensitivity to maximal CP violation ($\delta = 90°$) in the δm^2_{12} and θ_{13} parameter space, following the convention of [13], is plotted in Fig. 15.

The 3σ sensitivity to δ, having fixed $\delta m^2_{12} = 7.1 \cdot 10^{-5}$ eV^2, is shown in Fig. 16.

In case of a positive result the fit to the $p(\nu_e \to \nu_\mu)$ and to the p$(\overline{\nu}_e \to \overline{\nu}_\mu)$ probabilities can simultaneously determine θ_{13} and δ, see fig. 17. The net effect of the sign(Δm^2)ambiguity is to make undetectable sign$(\delta \cdot \text{sign}(\Delta m^2))$. This derives by the negligible matter effects at the 130 km, so that a change of sign$(\Delta m^2)$is equivalent to a change of the sign of δ. The $\theta_{23}/(\pi/2 - \theta_{23})$ ambiguity has no effect in this plot since the BetaBeam performances are computed for the central value of SuperKamiokande: $\theta_{23} = 45°$. This experimental setup has not strong handles (like the reconstruction of the neutrino energy) in order to reduce the correlations and degeneracies but the purpose of the experiments of this phase is not considered to be the precise measurements of all the parameters but a first attempt to access CP violation for values of θ_{13} which are large enough ($\theta_{13} \geq 3\,\text{deg}°$). This corresponds also to the two-steps logic of the T2K project, where the second phase aiming to the CP violation search is pending from a positive result on θ_{13} in the first phase. A detailed study on the degeneracies for the SPL superbeam and the Beta beam has been recently published [20].

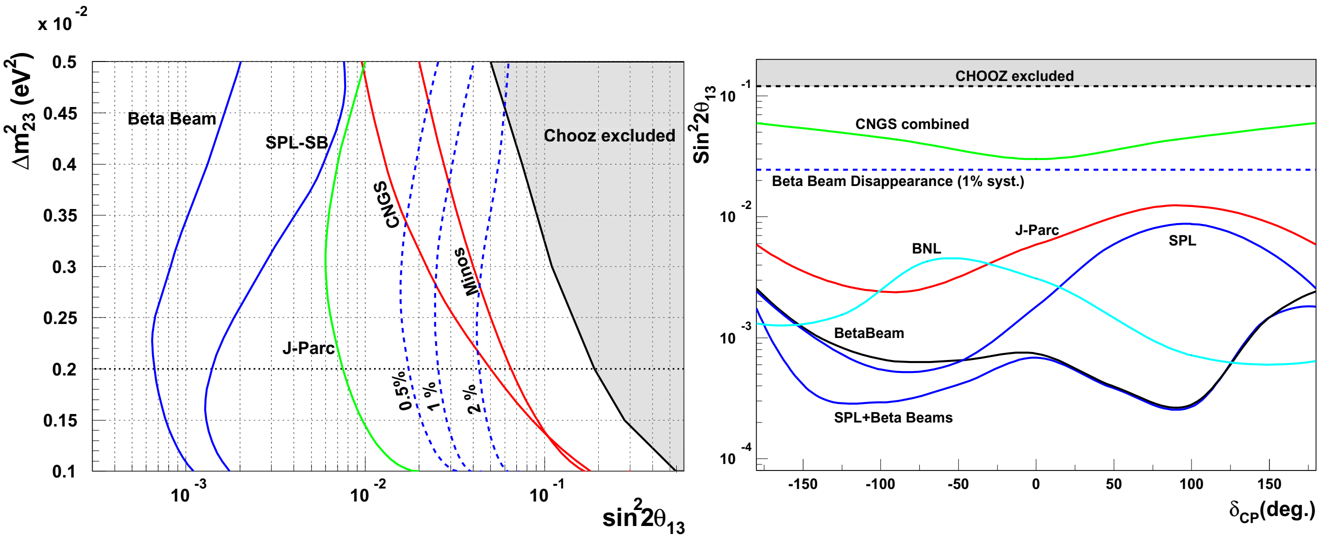

Figure 14: LEFT: 90%CL sensitivity of the disappearance channel to θ_{13} in a 5 yrs run drawn as dotted lines. The labels 0.5%, 1% and 2% indicate the systematic errors with which are computed. Also shown are the appearance sensitivities of Beta and SPL beams, computed for $\delta = 0$, sign(Δm^2)=+1. The combined CNGS limit is taken from ref. [14], J-Parc from [36], Minos from ref. [38]. RIGHT: 90%CL sensitivity expressed as function of δ for $\delta m^2_{23} = 2.5 \cdot 10^{-3} eV^2$. CNGS and J-Parc curves are taken from ref. [14], BNL from ref. [37]. All the appearance sensitivities are computed for sign$(\Delta m^2) = +1$.

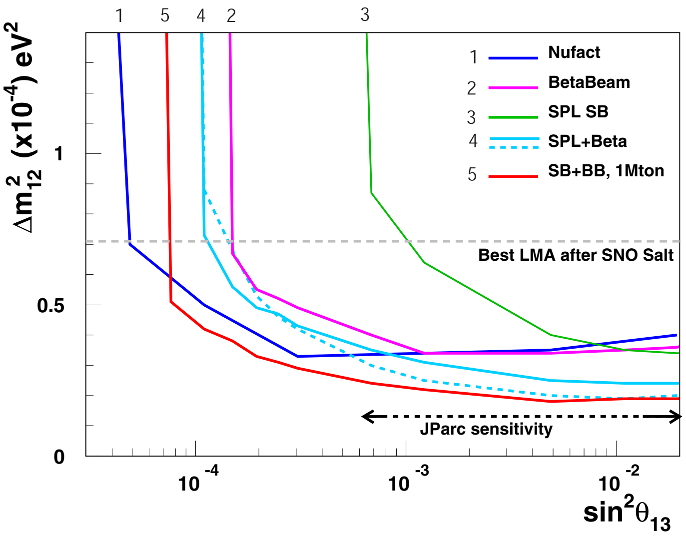

Figure 15: 99%CL δ sensitivity of the Beta Beam, of the SPL-SuperBeam, and of their combination, see text. Dotted line is the combined SPL+Beta sensitivity computed for sign(Δm^2)=-1. Sensitivities are compared with a 50 GeV Neutrino Factory producing $2 \cdot 10^{20} \mu$ decays/straight section/year, and two 40 kton detectors at 3000 and 7000 km [13].

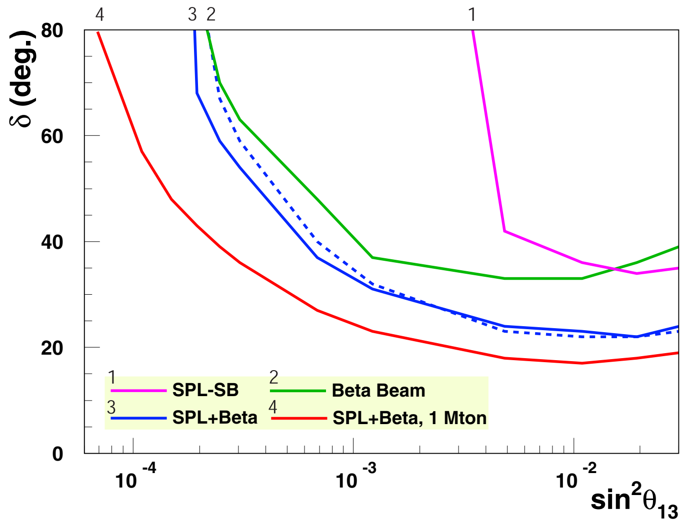

Figure 16: δ discovery potential (3σ) as function of θ_{13} . Dotted line are sensitivities computed for sign(Δm^2)=-1

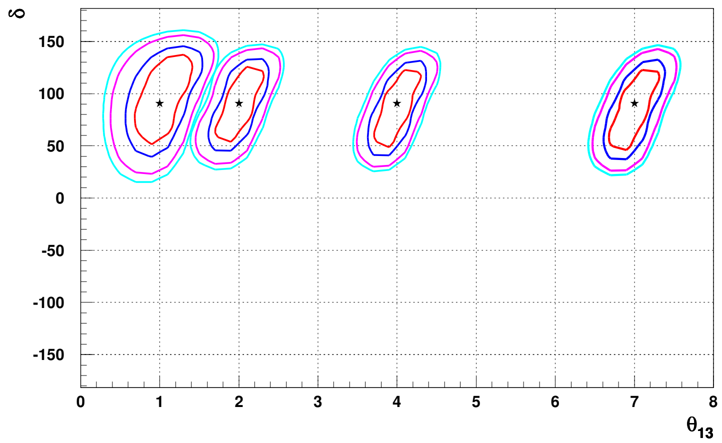

Figure 17: Fits to θ_{13} and δ after a 10 yrs BetaBeam run. Plots are shown for $\delta = 1^\circ, 2^\circ, 4^\circ, 7^\circ$. For the other neutrino oscillation parameters see the text. Lines show 1σ, 90%, 99% and 3σ confidence levels.

5 Precision measurements

The assessment of CP violation with precision measurements of the elements of the mixing matrix and the resolution of the mass hierarchy will characterize the experiments of the last phase.

Beta Beams could be a convenient tool for this kind of measurements by increasing the beam energy correspondingly the baseline. It has been shown by [5] that Beta Beams at high energy could achieve performances on the search for CP violation competitive to the ones of neutrino factories. The Beta Beam option considered so far for the Frejus detector was based on recycling part of the already existing equipments at CERN, like the SPS. The accelerations of the ions with the SPS is limited up to a $\gamma \leq 150$, due to the magnetic field achievable with the existing magnets. By refurbishing the SPS with super-conductive magnets ions could be accelerated up to ($\gamma \leq 600$). The optimal configuration would correspond to $\gamma = 350$ for ^{6}He and $\gamma = 580$ for ^{18}Ne, with $L = 732$ km. The advantages of this option, by considering a water Cerenkov detector of the same size as the one considered for the Frejus project but located in Gran Sasso, would consist in:

- The higher energy would allow to exit from the region where cross sections are strongly affected by nuclear effects and poorly known. By taking into account the flux focalization and the increase in cross section, the rate of ν_μCC events would increase by a factor 10.
- In this energy range the reconstruction of the energy spectrum becomes possible (the experiment is no more a merely counting experiment) and this information can be used in order to resolve correlations and degeneracies
- Matter effects become sizeable and can be used to measure the sign of Δm^2_{23}

Of course there would be also other technical aspects to deal with: the new SPS with superconductive magnets would have to provide a power of about 1 MW for the acceleration of the beam and also the magnets in the Decay ring would have to be replaced with superconductive magnets in order to keep its size reasonable.

Degeneracies can be resolved either combining different experiments with different E_ν/L or matter effects, or exploiting, whenever this is possible, the energy dependence of the signal within the same experiment. The energy dependence is particularly helpful for experiments performed with an "on-peak" baseline. Figure 18 compares the vacuum probabilities for $\nu_e \to \nu_\mu$ and $\bar{\nu}_e \to \bar{\nu}_\mu$ with $\theta_{13} = 6^\circ$ and $\delta = 40^\circ$ to those of the intrinsic-degenerate solution at $\langle E_{\nu(\bar{\nu})}\rangle$. The neutrino and anti-neutrino probabilities cross at the $\langle E_{\nu(\bar{\nu})}\rangle$, but are quite different at other energies. Thus spectral information can definitely help in disentangling them provided to have a sufficient energy resolution.

This is shown quantitatively in figure 19, where the results of a simultaneous fit of δ θ_{13} are presented for 10 years exposure of: a 400 Kton water Cerenkov detector at a baseline of 130 Km and $\gamma = 60$ for ^{6}He and $\gamma = 100$ for ^{18}Ne (Setup I); a 40 Kton and a 400 Kton detectors at a baseline of 732 Km and $\gamma = 350$ for ^{6}He and $\gamma = 580$ for ^{18}Ne (Setup II); and a 400

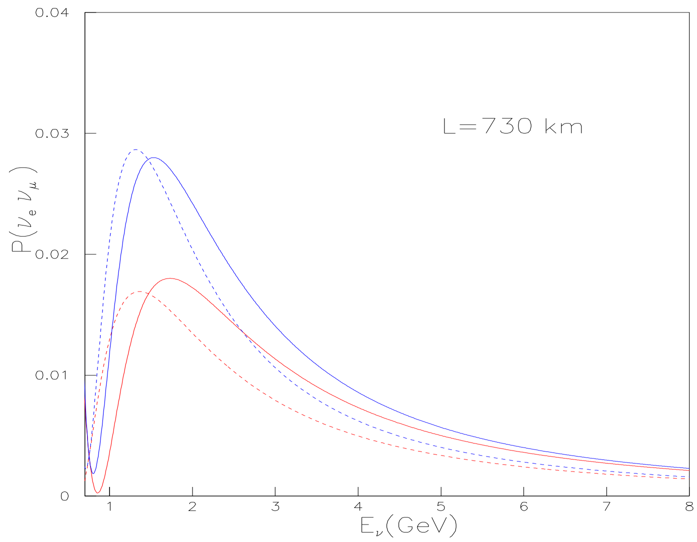

Figure 18: $P(\nu_e \to \nu_\mu)$ and $P(\bar{\nu}_e \to \bar{\nu}_\mu)$ as a function of the energy in GeV, at $L = 730$ km, for $\theta_{13} = 6°$ and $\delta = 40°$ (solid) and for the degenerate solution at $\theta'_{13}(\langle E_\nu \rangle), \delta'(\langle E_\nu \rangle)$ with $\langle E_\nu \rangle = 1.5$ GeV (dashed).

Kton detector located at 3000 Km with $\gamma = 1500$ for ^{6}He and $\gamma = 2500$ for ^{18}Ne (acceleration of the ions performed with LHC) (Setup III). Considering the same detector, there is a large improvement in the accuracy of the fit between Setup I and Setup II. The intrinsic degeneracies present for the low-energy option, they tend to get resolved in Setup II, even with a detector 10 times smaller.

Given the introduction of sizeable matter effects in Setup II, the sign(Δm^2_{23}) becomes measurable simultaneously with θ_{13} and δ for $\theta_{13} \geq 3°$ (see Fig. 20).

Neutrino factories [9, 10, 12, 13] will constitute the ultimate tool for the study of neutrino oscillations and the precise measurement of the mixing matrix elements and mass hierarchy. As Beta Beams, they overcome the major difficulty of conventional neutrino beams based on pion and kaon decays: the purity of the beam and the modelization of the fluxes.

Neutrinos will be generated in this case from the decays of muons circulating in a storage ring ($\nu_e$and $\overline{\nu}_\mu$from the decays of $\overline{\mu}$or $\overline{\nu}_e$and $\nu_\mu$from the decays of μ) and can be known at 10^{-3} level. The beam, other than by its purity is also characterized by a very high flux, as shown in table refcompflux.

The most straigthforward way of exploiting this beam is to search for $\nu_\mu \leftrightarrow \nu_e$oscillations by looking at the appearance of wrong sign muons in a large magnetized iron detector (the so called Golden Channel). The beam is intrinsically pure and backgrounds can be kept at the 10^{-4} level by rejecting neutrino interaction events with low energy muons. The use of a beam

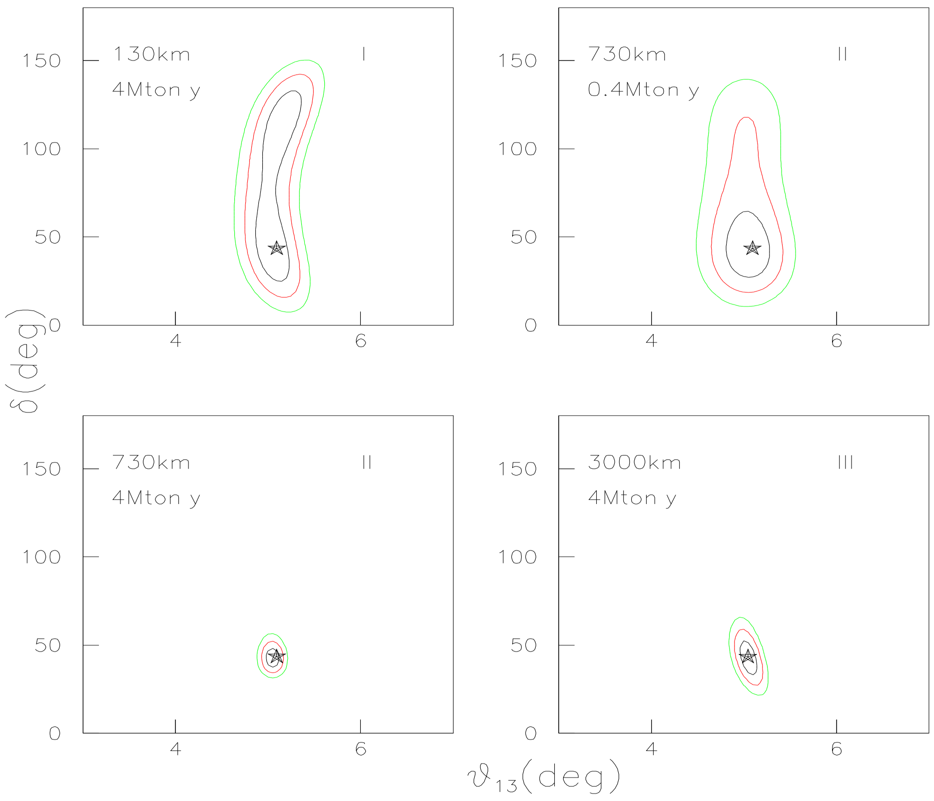

Figure 19: 1,2,3σ contours on the plane (θ_{13}, δ) in the setups I, II for the 40kton and 400 kton detectors and for setup III. The input values of the parameters are indicated by a star.

produced from about 2×10^{21} decays of 50 GeV muons with a 40 Kton detector located at 3000 Km allows to achieve unprecedented sensitivities on θ_{13}, δ_C, sign(Δm^2_{23}) and to measure the atmospheric neutrino oscillation parameters θ_{23} and Δm^2_{23} respectively at the 10% and 1% level. The sensitivity on θ_{13} can be pushed down to $\sin^2\theta_{13} \leq 10^{-5}$ $(0.1°)$, this is actually the only possible way to be sensitive to so low values of θ_{13}.

The search for CP violation is performed by measuring the asimmetry among the $\nu_e \to \nu_\mu$ and $\nu_e \to \overline{\nu_\mu}$ oscillation probabilities. Matter effects can produce the same asymmetry. They can be easely used at neutrino factories for baselines larger than about 1000 km in order to measure sign(Δm^2_{23}) but they interfere with the measurement of CP violation until baselines of about 2000 km, after which they become dominant 21. For the CP search matter effects have to be subtracted once determined the sign(Δm^2_{23}), this can be done with a 2% accuracy. This subtraction has to be performed in bins of the reconstructed neutrino energy given the different energy behavior matter effects and CP violation.

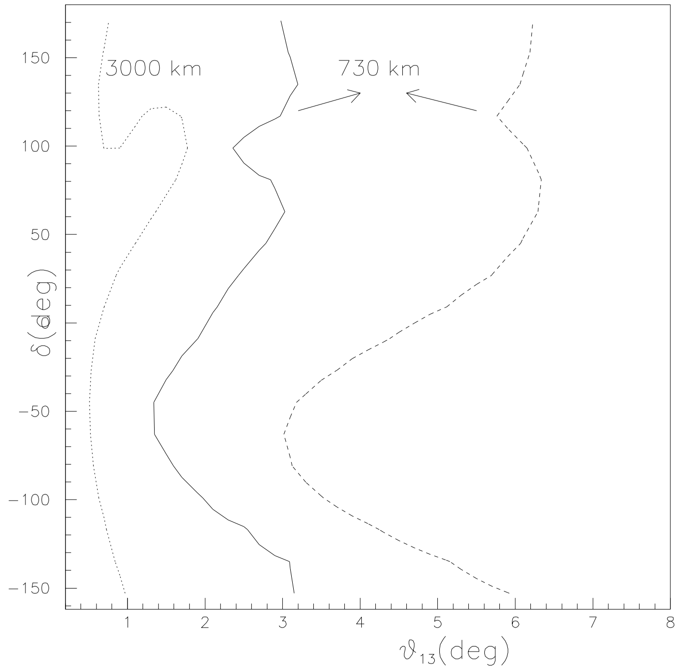

Figure 20: Regions where the true sign(Δm^2_{23}) $= +1$ can be measured at 99% CL (ie. no solution at this level of confidence exists for the opposite sign). The lines correspond to setup II with the 400kton water Cerenkov (solid), the 40kton one (dashed) and to setup III (dotted).

The correlation among θ_{13} and δ_C in the simultaneous fit of the oscillation probabilities for neutrinos and antineutrinos is particularly strong at short baselines. The optimal choice for the CP search is for a baseline around 3000 Km. The accuracy can be increased by combining measurements at different baselines 22.

The best way to reduce correlations and ambiguities is to combine the observation of the golden channel with the one of the "Silver channel" ($\nu_e \leftrightarrow \nu_\tau$oscillations). $\nu_e \leftrightarrow \nu_\tau$oscillations have a opposite CP behavior than $\nu_e \rightarrow \nu_\mu$ oscillations. This can be easely understood by considering that for $\nu_e$the sum of the survival probability and the two oscillation probabilities (in $\nu_\mu$and ν_τ) is 1. The combination of the measurement of wrong sign muons at 3000 Km with $\nu_e \leftrightarrow \nu_\tau$oscillations at 730 Km (a 4Kton OPERA-like detector) solves the ambiguities and eliminates the clone regions 23.

A comparison of the sensitivities of neutrino factories for the measurements of θ_{13} and δ_C with respect to other possible neutrino facilities is shown in figures 24.

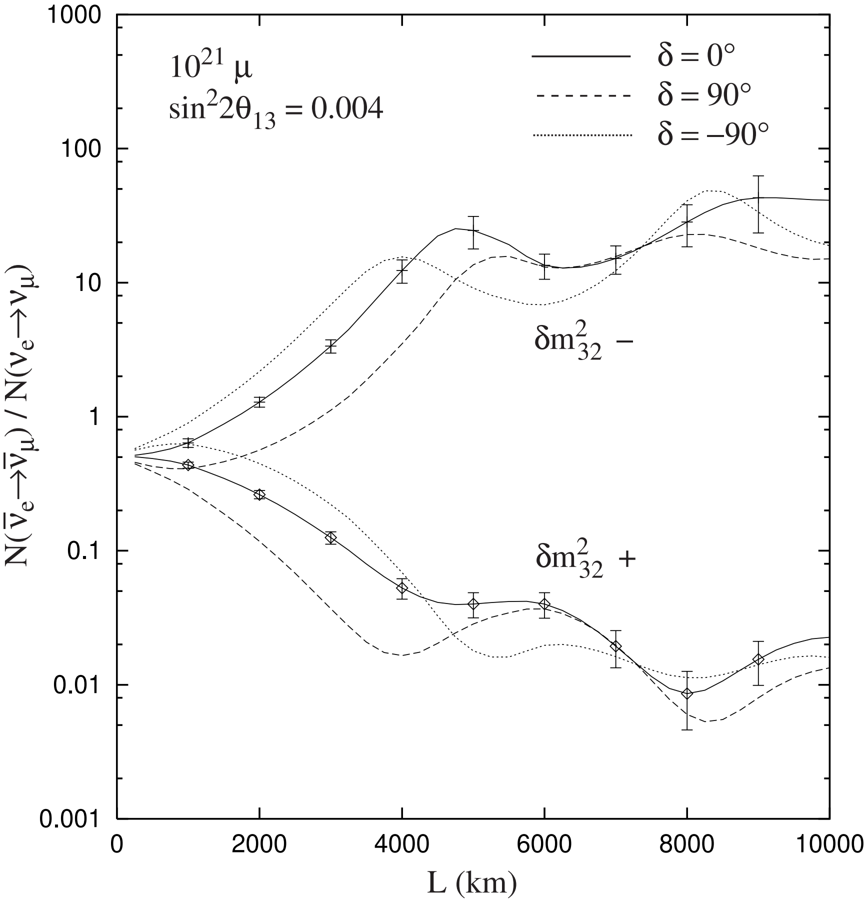

Figure 21: *Ratio of the oscillation probabilities of neutrinos and antineutrinos as a function of the baseline. The different lines correspond to values of the CP-violating phase δ of* $0°$, $90°$ *and* $-90°$. *After about 1000 km, matter effects dominate over CP violation. Around 7500 km CP violation effects go to zero.*

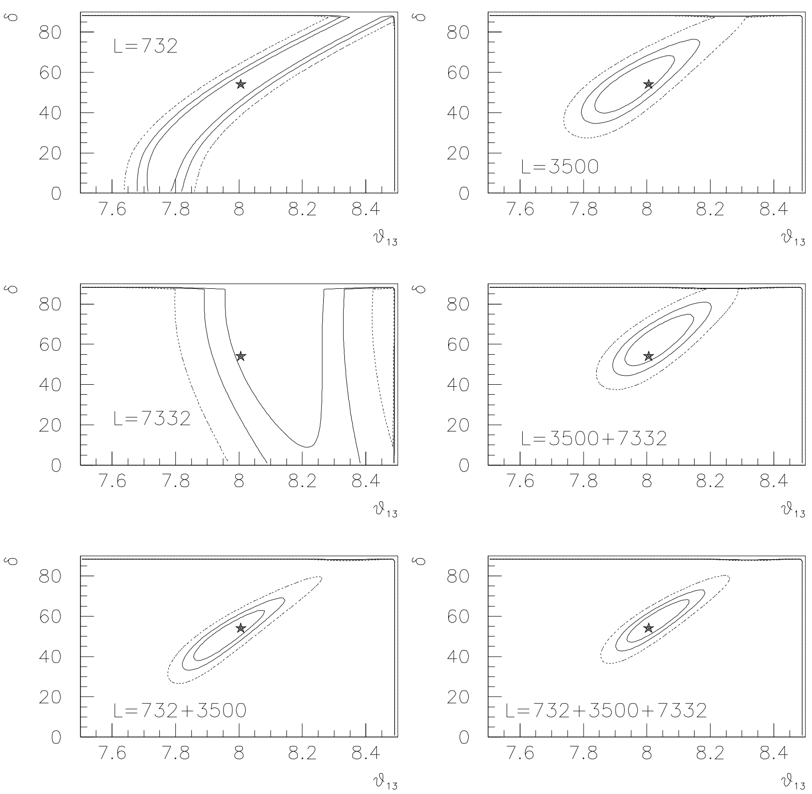

Figure 22: *Correlations in a simultaneous fit of θ_{13} and δ, using a neutrino energy threshold of about 10 GeV. With a single baseline correlations are quite strong, they can be reduced by combining informations from different baselines. techniques [10].*

Beam	E_ν (GeV)	Flux ($\nu/m^2/yr$)	L (Km)	CC ($\nu/Kton/yr$)
CNGS	17.7	$3.5 \cdot 10^{11}$	730	2448
T2K1	0.7	$1.9 \cdot 10^{11}$	295	95
T2K2	0.7	$1.2 \cdot 10^{12}$	295	570
SPL	0.27	$4.78 \cdot 10^{11}$	130	31.1
Beta B	0.36	$1.88 \cdot 10^{11}$	130	24.5
NUFACT	30	$2.4 \cdot 10^{12}$	3000	17700

Table 5: Comparison of the fluxes and CC event rates of various neutrino facilities

References

[1] G. Gratta, Neutrino 2004 Conference 14-19 June 2004, Paris.

[2] T. Nakaya, Neutrino 2004 Conference 14-19 June 2004, Paris.

[3] M. Maltoni et al., hep-ph/0405302

[4] T. Schwetz., hep-ph/0311217

[5] J.Burguet-Castell et al., hep-ph/0312068.

[6] J.Bouchez et al., hep-ph/0310059.

[7] P. Zucchelli, Phys. Lett. B **532** (2002) 166.

[8] M. Mezzetto, J.Phys.G29:1771-1776, 2003; hep-ex/0302005.

[9] M. Apollonio et al., CERN TH-2002-208, hep-ph/0210192.

[10] A. Cervera et al., hep-ph/0002108.

[11] D. Autiero et al., hep-ph/0305185.

[12] C. Albrigth et al., hep-ph/0008064.

[13] J. Burguet-Castell *et al.*, Nucl. Phys. B **608**, 301 (2001) [arXiv:hep-ph/0103258].

[14] P. Migliozzi and F.Terranova, hep-ph/0302274.

[15] M. Komatsu et al., hep-ph/0210043.

[16] J.Burguet-Castell et al., hep-ph/0103258.

[17] Minakata et al., hep-ph/0108085.

[18] V. Barger et al., hep-ph/0112119.

[19] A. Donini et al., hep-ph/0312072.

[20] A. Donini et al., hep-ph/0406132.

[21] M. Freund., hep-ph/0103300.

[22] P. Hubner et al., hep-ph/0403068.

[23] E. Akhmedov et al., hep-ph/0402175.

[24] P. Hubner et al., hep-ph/0303232.

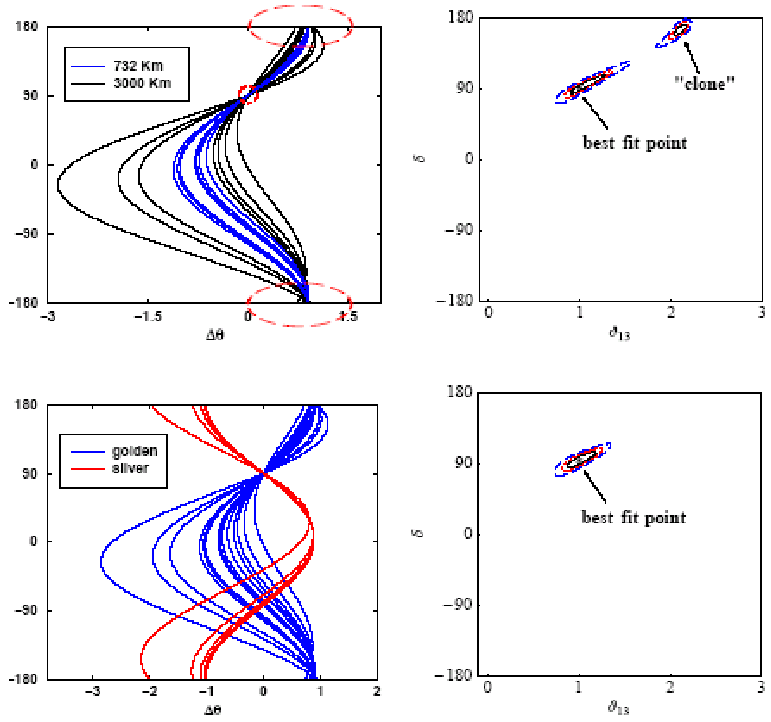

Figure 23: *Curves of equal oscillation probability in the $\delta, \Delta\theta$ plane (where $\Delta\theta$ is the difference between θ_{13} and its nominal value of $1°$), for the golden channel at two different baselines and for the golden+silver channel at the same two baselines. The curves, generated for different energy bins, all meet at the nominal value of the parameters.*

[25] F. Ardellier et al., hep-ph/0405032.
[26] K. Anderson et al., hep-ph/0405032.
[27] Y. Hayato et al., Letter of intent, neutrino oscillation experiment at JHF.
[28] I. Ambats et al., NOVA proposal (P929)
[29] M. Mezzetto, Proceedings of the 2nd NO-VE workshop, Venice, December 3-5, 2003
[30] M. Lindner, Proceedings of the 2nd NO-VE workshop, Venice, December 3-5, 2003
[31] V. Migliozzi, Proceedings of the 2nd NO-VE workshop, Venice, December 3-5, 2003
[32] J. Bouchez, Proceedings of the 2nd NO-VE workshop, Venice, December 3-5, 2003
[33] K. Nishikawa, Proceedings of the 2nd NO-VE workshop, Venice, December 3-5, 2003
[34] P. Huber et al., *Nucl. Phys.* **B654** (2003) 3
[35] V. Barger et al., *Phys. Lett.* **B560** (2003) 75
[36] Y. Itow *et al.*, "The JHF-Kamioka neutrino project,", hep-ex/0106019.
[37] M. V. Diwan *et al.*, Phys. Rev. D **68**, 012002 (2003) [arXiv:hep-ph/0303081].
[38] Tzanakos, NuFact 03 Conference Proceedings

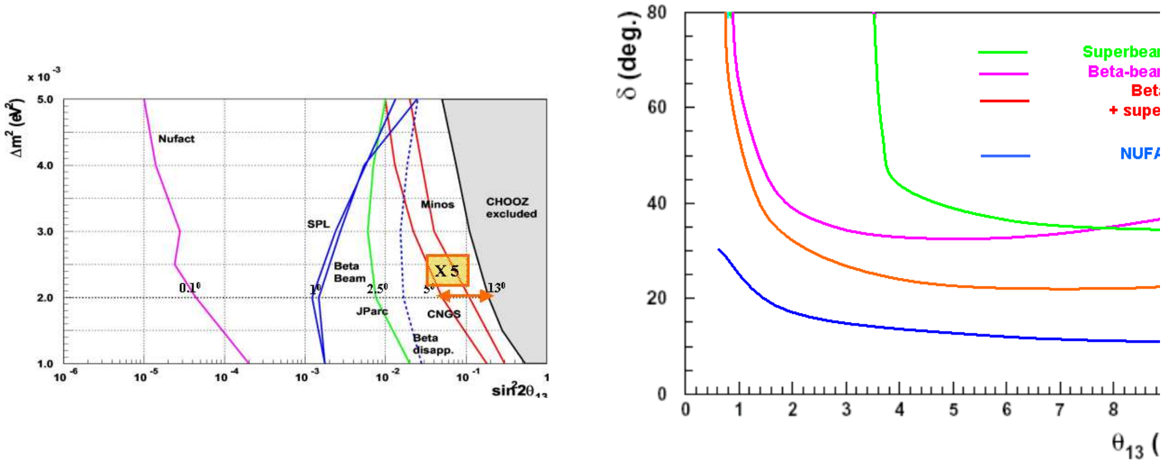

Figure 24: Sensitivities for θ_{13} and δ_{CP} for a neutrino factory compared to other projects.